Acta Physiologiae Plantarum (2022) 44:129
https://doi.org/10.1007/s11738-022-03464-w

ORIGINAL ARTICLE

Cellular and ultrastructural alterations of *Arabidopsis thaliana* roots in response to exogenous *trans*-aconitic acid

Kátia Aparecida Kern-Cardoso[1] · Marcio Shigueaki Mito[1] · Adela María Sánchez-Moreiras[2] · Manuel Joaquín Reigosa[2] · Emy Luiza Ishii-Iwamoto[1]

Received: 1 September 2020 / Revised: 7 April 2021 / Accepted: 24 September 2022 / Published online: 7 October 2022
© The Author(s) 2022

Abstract

In this work, the responses of *Arabidopsis thaliana* (L.) Heynh to *trans*-aconitic acid (TAA) were investigated. *A. thaliana* was grown in the presence of TAA in a concentration range of 400–1200 µM for 7 or 15 days. Changes in the morpho-anatomy, cellular ultrastructure, and micromorphology of the roots were evaluated by light and transmission electron (TEM) microscopy. At concentrations below 1000 µM, TAA reduced the length of the primary roots, but induced an early appearance of lateral roots and root hairs. At a concentration of 1200 µM, TAA suppressed the growth of seedlings. The images of longitudinal sections of root tips of seedlings treated with IC_{50} of TAA (684 µM) revealed a reduced elongation zone with an increased differentiation zone. TEM images showed an increase in the number and volume of vacuoles, an increase in vesicles containing electron-dense material derived from plasmalemma, and electron-dense granules attached to the cell wall. *Trans*-aconitic acid induced an early differentiation of *A. thaliana* seedlings suggesting an interference in the auxin action. Changes in the cellular ultrastructure may represent vacuolar and extracellular accumulation of TAA, to remove excess TAA in the cytosol and mitochondria. An inhibition of aconitase and the chelation of intracellular cations may have contributed to cytotoxicity of TAA at 1200 µM concentration.

Keywords Organic acid · Auxin · Weed · Root system · Seedling · Crop protection

Introduction

Trans-aconitic acid (TAA) [(E)-1-propene-1,2,3-tricarboxylic acid], a natural isomer of the tricarboxylic acid cycle (TCA) intermediate *cis*-aconitate, occurs in nature in sugar-containing plants, such as sugar cane (*Saccharum officinarum* L.), wheat (*Triticum aestivum* L.) (Thompson et al. 1997), maize (*Zea mays* L.) (Brauer and Teel 1982), and sweet sorghum (*Sorghum bicolor* L.*)* (Klasson 2017).

Trans-aconitic acid is also present in the forage species *Urochloa* sp. (Voll et al. 2004; Brum et al. 2009) and in medicinal plants, such as *Asarum europaeum* (Krogh 1971). It is also produced by bacteria of the genus *Pseudomonas* (Yuhara et al. 2015).

Trans-aconitic acid is synthesized by the interconversion between *cis*-aconitate and TAA, mediated by aconitate isomerase in both microbes and plants (Klinman and Rose 1971; Thompson et al. 1990), and by the dehydration of citric acid in plants catalyzed by citrate dehydratase (Brauer and Teel 1981, 1982). Although closely related to the TCA cycle, TAA is an effective inhibitor of mitochondrial and cytosolic aconitase and thus it is compartmentalized in vacuoles (Saffran and Prado 1949; Eprintsev et al. 2015).

The role of TAA in plants is not clear, but there is evidence that it acts as an antifeedant, (Katsuhara et al. 1993), in resistance against diseases (Kidd et al. 2001; Rémus-Borel et al. 2006) and in aluminum resistance (Kidd et al. 2001; Wenzl et al. 2002; Mariano and Keltjen 2003). The role of TAA and its methylated derivative as a phytoalexin has also been suggested based on its antifungal activity against

Communicated by W. Zhou.

✉ Adela María Sánchez-Moreiras
adela@uvigo.es

✉ Emy Luiza Ishii-Iwamoto
eliiwamoto@uem.br

[1] Department of Biochemistry, State University of Maringá, Maringá 87020900, Brazil

[2] Departamento de Biolox a Vexet e Ciencia do Solo, Facultade de Biolox, Universidade de Vigo, a.36310 Vigo, Spain

Cladosporium cucumerinum (Rémus-Borel et al. 2006), in Si amendment, and in pathogen resistance in wheat plants (Rémus-Borel et al. 2009). A nematicidal effect of TAA synthesized by *Bacillus thuringiensis* has been suggested by Du et al. (2017). These bioactivities suggest a great potential of TAA and its methylated derivative in crop protection.

Because TAA can be extracted with high yields and purity from sugar cane molasses, which contains 0.5–3.0% of TAA (Dorman et al. 2015), its use for industrial purposes has been proposed, such as in the production of biodegradable polyesters (Dorman et al. 2015). However, studies on the effects of exogenous TAA on plants are scarce.

Herbicidal action has been suggested based on the suppressive action on the emergence of some weeds including *Ipomoea grandifolia* (Dammer) O'Donell, *Bidens pilosa* L., *Euphorbia heterophylla* L., and *Sida rhombifolia* L. (Voll et al. 2010; Foletto et al. 2012). Phytotoxicity of exogenous TAA in the soybean has been reported by Coelho-Bortolo et al. (2018) but at higher doses of TAA than those reported in weeds. Although TAA is an efficient inhibitor of mitochondrial aconitase, inhibition of *I. grandifolia* is not related to inhibition of enzyme activity, since root apex respiration and respiration driven by citrate oxidation in mitochondria isolated from the roots of *I. grandifolia* are not altered by TAA (Foletto et al. 2012).

Alterations in seedling growth by phytotoxicants added to the soil are generally associated with changes in the root system, which can be observed in the cellular ultrastructure. *Arabidopsis thaliana* (L.) Heynh, an herbaceous plant of the Brassicaceae family, has been widely used as a model plant for studies on the regulation of root development, the responses to nutritional changes, and the effects of natural and synthetic compounds (Pang and Meyerowitz 1987; Williamson et al. 2001; Rahman et al. 2002; Müller and Schmidt 2004; Petersson et al. 2009; Pelagio-Flores et al. 2012; Kellermeier et al. 2014; Sánchez-Moreiras et al. 2018).

In the context of the potential utilization of TAA for agricultural purposes, in this work we investigated the mode of action of exogenous TAA by examining changes in morpho-anatomy, cellular ultrastructure, and micromorphology in roots of *A. thaliana* seedlings.

Materials and methods

Plant material and growth conditions

Seeds of *A. thaliana* (L.) Heynh., ecotype Columbia (Col-0), were surface-sterilized with 50% ethanol (3 min) and 0.5% sodium hypochlorite (3 min), both in 0.01% Triton, and washed three times with distilled water. Subsequently, the seeds were vernalized in 0.1% agar (*w*/*v*) at a temperature of 4° C, for 48 h, and then transferred to the top of square Petri dishes (100 × 15 mm) containing 0.8% agar (*w*/*v*) supplemented with macro- and micronutrients (Murashige–Skoog basal medium, M5519 Sigma-Aldrich) and 1% sucrose (*w*/*v*); the pH was adjusted to 6.0.

The stock solutions of *trans*-aconitic acid were dissolved in distilled water, adjusted to pH 7.0 with KOH, then added to the agar at the proportion of 0.1% (v/v) to obtain the final concentrations of 400, 600, 800, 1000 and 1200 µM. For each concentration, 24 seeds were sown per square dish under a laminar flow hood, the dishes were sealed with "Leukopor" (BSN Medical) and placed upright in a growth chamber for promoting geotropism, at a temperature of 22 °C, a photoperiod of 8 h light (120 µmol/m^2s), and a relative humidity of 55%. After 15 days, the primary root length was measured and the dose–response curve was used to calculate the IC_{50} for root growth inhibition. Seedlings treated with IC_{50} TAA for 7 and 15 days were randomly selected to photograph the whole root structure in an Olympus SZX9 stereoscopic microscope.

Light and transmission electron microscopy (TEM) of longitudinal sections of *Arabidopsis* roots

In total, 40 roots of *A. thaliana* grown in the absence (control) or presence of the IC_{50} of TAA for 7 and 15 days were used for microscopic studies. The apical meristems, approximately 0.5 cm, were cut, immersed in 0.1 M cacodylate buffer (pH 7.2) with 5% glutaraldehyde fixative, and incubated for 4 h. Subsequently, three washes of 4 h each were performed with 0.1 M cacodylate buffer (pH 7.2). After washing, the samples were immersed in 0.1 M cacodylate buffer with 2% osmium tetroxide for 3 h and in 10% acetone with 2% uranyl for 1 h. For dehydration, the samples were immersed in increasing dilutions of acetone: 50% acetone (2 × 30 min), 75% acetone (2 × 1 h), 80% acetone (2 × 1 h), 95% acetone (2 × 1 h), and 100% acetone (2 × 2 h). After this, impregnation was started in the rotor with Spurr resin: 1:3 Spurr in acetone (3 × 2 h), 2:2 Spurr in acetone (3 × 2 h), and 3:1 Spurr in acetone (2 × 2 h + 3 × 1 h); all dehydration and impregnation steps were carried out at 4 °C.

Inclusion in Spurr resin was performed in the rotor at room temperature. Subsequently, the samples were placed in resin molds and heated in an oven at 60 °C for 2 days. Semi-fine cuts of 0.7 µm and ultrathin cuts of 50–70 nm were done for light and electron microscopy, respectively.

The semi-fine sections were stained with toluidine blue and observed under a Nikon Eclipse 800 light microscope attached to a Nikon DS-U2 digital camera with the NIS-Elements D 2.30 SP1 software.

The ultrathin sections were collected on copper grids of 100 and 200 "mesh" and contrasted with uranyl acetate (2%) for 30 min and with lead citrate (Reynolds 1963) for 12 min (2-min washes with ultrapure water were done after each

step). Ultrathin sections were observed with a TEM JEOL JEM-1010 (100 kV) (Peabody, MA, USA) equipped with an Orius-CCD digital montage plug-in camera (Gatan Inc., Gatan, CA, USA) and a Gatan Digital micrograph software (Gatan, Inc.).

Statistical analysis

All the experiments were carried out in a completely randomized design with five replications for dose–response curve. The data were expressed as mean ± standard error (S.E.) and analyzed using analysis of variance (ANOVA). Significant differences between means were identified by Duncan's multiple range test, and $P \leq 0.05$ was adopted as the minimum criterion of significance. The IC_{50} values were calculated by numerical interpolation through a cubic spline function of GraphPad Prism 5 software. Statistical analyses were performed using the Statistic™ software package.

Results

Root morphology

Representative images of *A. thaliana* seedlings grown in the absence (control) or presence of TAA at a concentration range of 400–1200 µM for 15 days are shown in Fig. 1. *Trans*-aconitic acid significantly altered root morphology, inducing a reduction of primary root length along with an increase in the number of lateral roots. At the highest concentration of 1200 µM, the development of both aerial parts and roots was extremely reduced compared with the untreated seedlings. Figure 2 shows the dose-dependent reduction in the length of primary roots with an IC_{50} of 684.31 µM.

Stereoscopic microscope images of root tips from 7- and 15-day-old untreated seedlings (Fig. 3a, c, e, g) show well-characterized differentiation and elongation zones, with a progressive development of root hairs in the differentiation

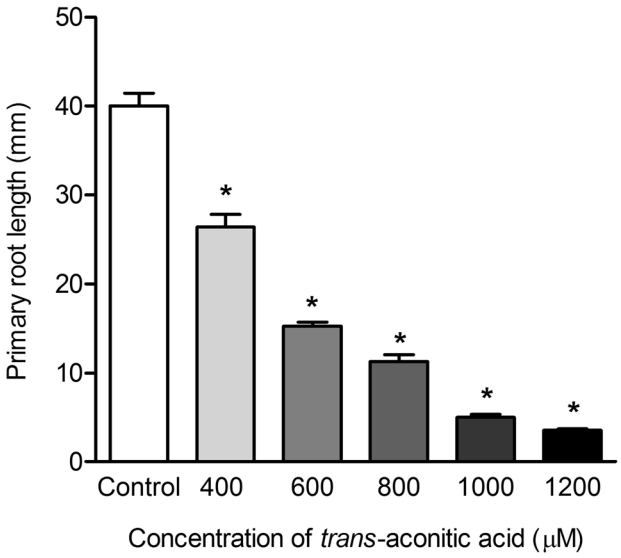

Fig. 2 Dose–response curves of the effect of *trans*-aconitic acid on the length of primary roots of *A. thaliana* at the 15th days of treatment. Values are means ± standard error of 5 series of independent experiments. The significant differences between the mean values of the treatments and the controls are indicated by asterisks and identified by analysis of variance with a Duncan's test ($P < 0.05$)

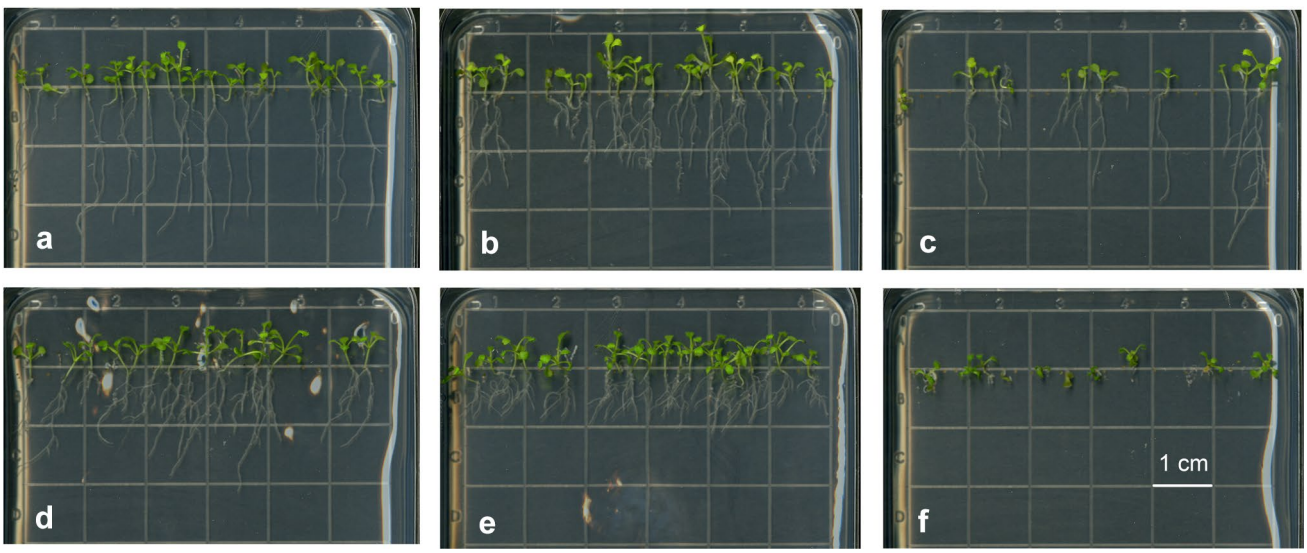

Fig. 1 *A. thaliana* seedlings grown for 15 days in the absence (control, **a**) and presence of 400 µM (**b**), 600 µM (**c**), 800 µM (**d**), 1000 µM (**e**) and 1200 µM (**f**) *trans*-aconitic acid

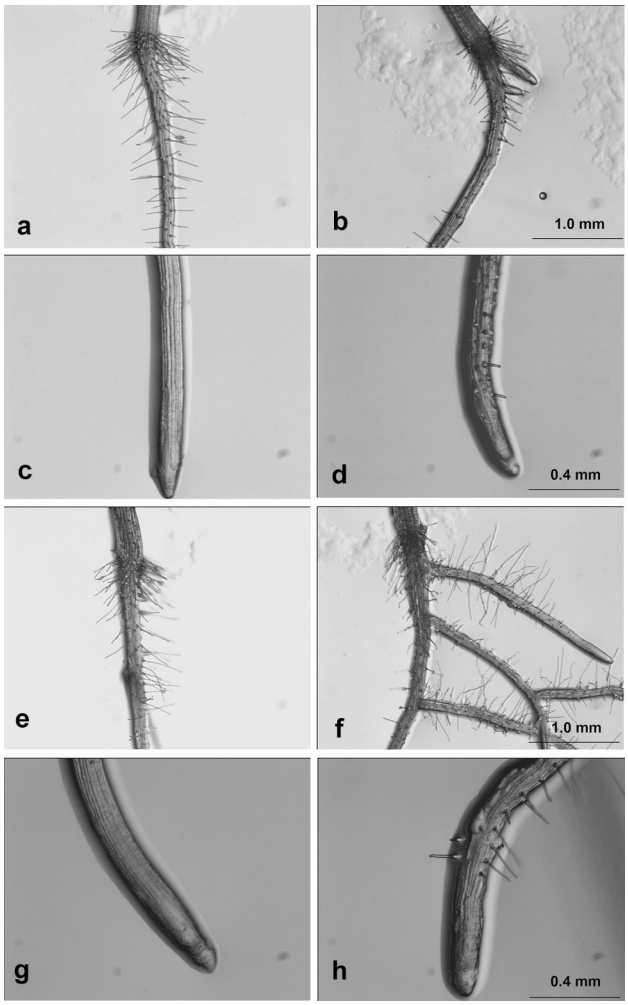

Fig. 3 Stereoscopic images of root tips of *A. thaliana* grown in the absence or presence of IC_{50} *trans*-aconitic acid (684 µM). Plants grown for 7 days: control (**a**, **c**) and *trans*-aconitic acid (**b**, **d**). Plants grown for 15 days: control (**e**, **g**), *trans*-aconitic acid (**f**, **h**)

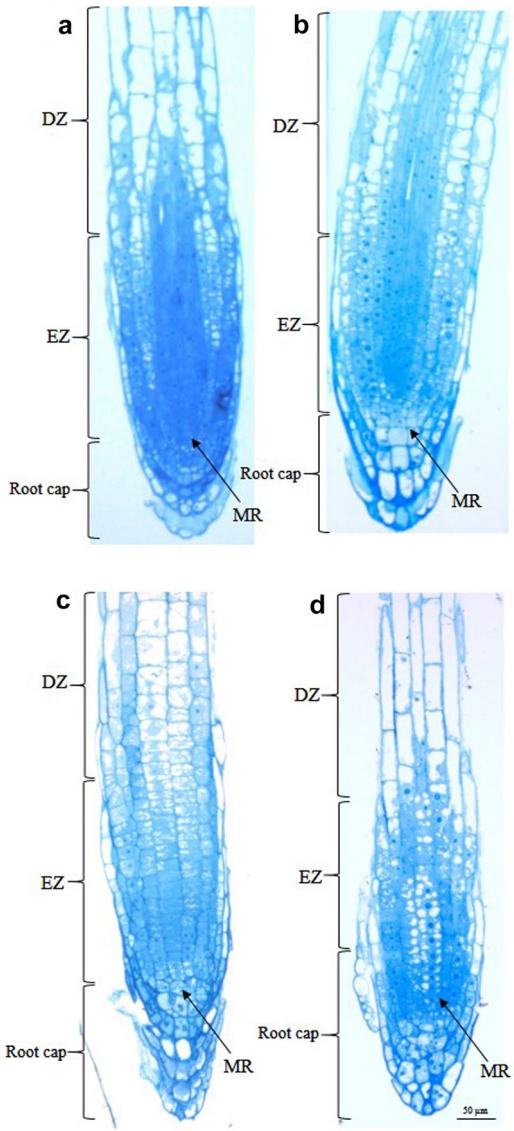

Fig. 4 Median longitudinal section of root tips from *A. thaliana* grown in the absence or presence of the IC_{50} *trans*-aconitic acid (684 µM). Plants grown for 7 days: control (**a**), *trans*-aconitic acid (**b**). Plants grown for 15 days: control (**c**), and *trans*-aconitic acid (**d**). *MR* meristematic zone, *EZ* elongation zone, *DZ* differentiation zone

zones. Seedlings treated with IC_{50} TAA (684 µM) for 7 days exhibited a precocious initiation of lateral roots and a reduction in the number and length of root hairs (Fig. 3b, d). Different from the root tip of control seedlings, TAA-treated seedlings exhibited bulges of root hairs near the root tip (Fig. 3d). After 15 days of treatment a highly branched root system with an abundance of long hairs in the lateral roots was observed (Fig. 3f, h). The root tip exhibited asymmetric rows of cells and ectopic root hairs, which were longer compared with those found at the 7th day of treatment (Fig. 3b, d).

The longitudinal sections of roots observed by light microscopy (Fig. 4) showed that treatment with TAA did not cause significant changes in the tissue organization in the root cap, elongation, and differentiation zones when compared with the control (Fig. 4a, c) with symmetric rows of cells. There was, however, a clear change in the division pattern of root zones, with a relative reduction in the elongation zone and a consequent increase in the differentiation zone. These findings were observed on the 7th day (Fig. 4b) and on the 15th day of treatment with TAA (Fig. 4d).

Root cell ultrastructure

Comparison of the ultrastructural analysis of root tip cell structure and organization in seedlings of *A. thaliana* grown for 7 or 15 days in the absence (Figs. 5, 6) or presence of TAA (Figs. 7, 8) revealed modifications in different cell organelles, particularly in vacuoles and

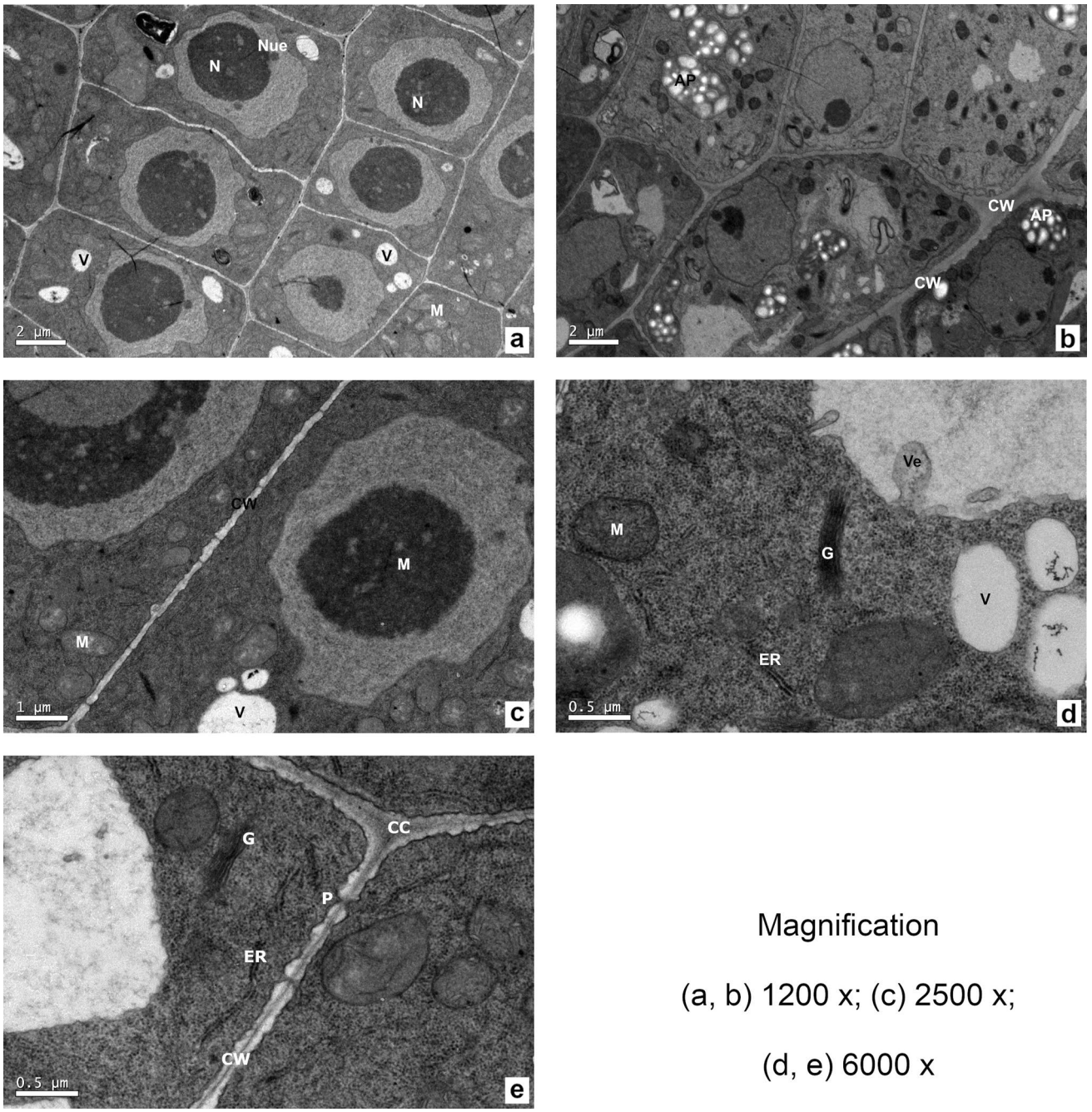

Fig. 5 TEM micrographs of root tip cells from a 7-day-old *A. thaliana* seedling (Control), showing a complete cell with centrally located nucleus (**a**, **c**), nucleus with one or two nucleoli (**a**, **b**), a number of small vacuoles (**a**, c), mitochondria of various shapes (**a**–**c**), vesicles (**d**) amyloplasts (**b**), endoplasmic reticulum (**d**, **e**), Golgi apparatus (**d**, **e**), cell wall with plasmodesmata (**e**). *AP* Amyloplasts, *CC* cell corners, *CW* cell wall, *ER* endoplasmic reticulum, *G* Golgi apparatus, *M* mitochondria, *Nue* nucleoli, *N* nucleus, *V* vacuoles, *Ve* vesicles, *P* plasmodesmata

mitochondria, and the appearance of electron dense materials in intracellular vesicles or in the cell corners. In both 7- and 15-day-old seedlings, an increased number of vacuoles containing dense granular material were observed in the cytosolic space. In the interspace between cell wall and plasma membrane, it was found a high number of vesicles, indicating increased secretory activity. In addition, cell corners appeared swollen compared to the control and rich in electron-dense deposits.

Increased numbers of mitochondria with variable shapes were observed in 7-day-old TAA-treated cells, including large and extended mitochondria, characteristic of dividing

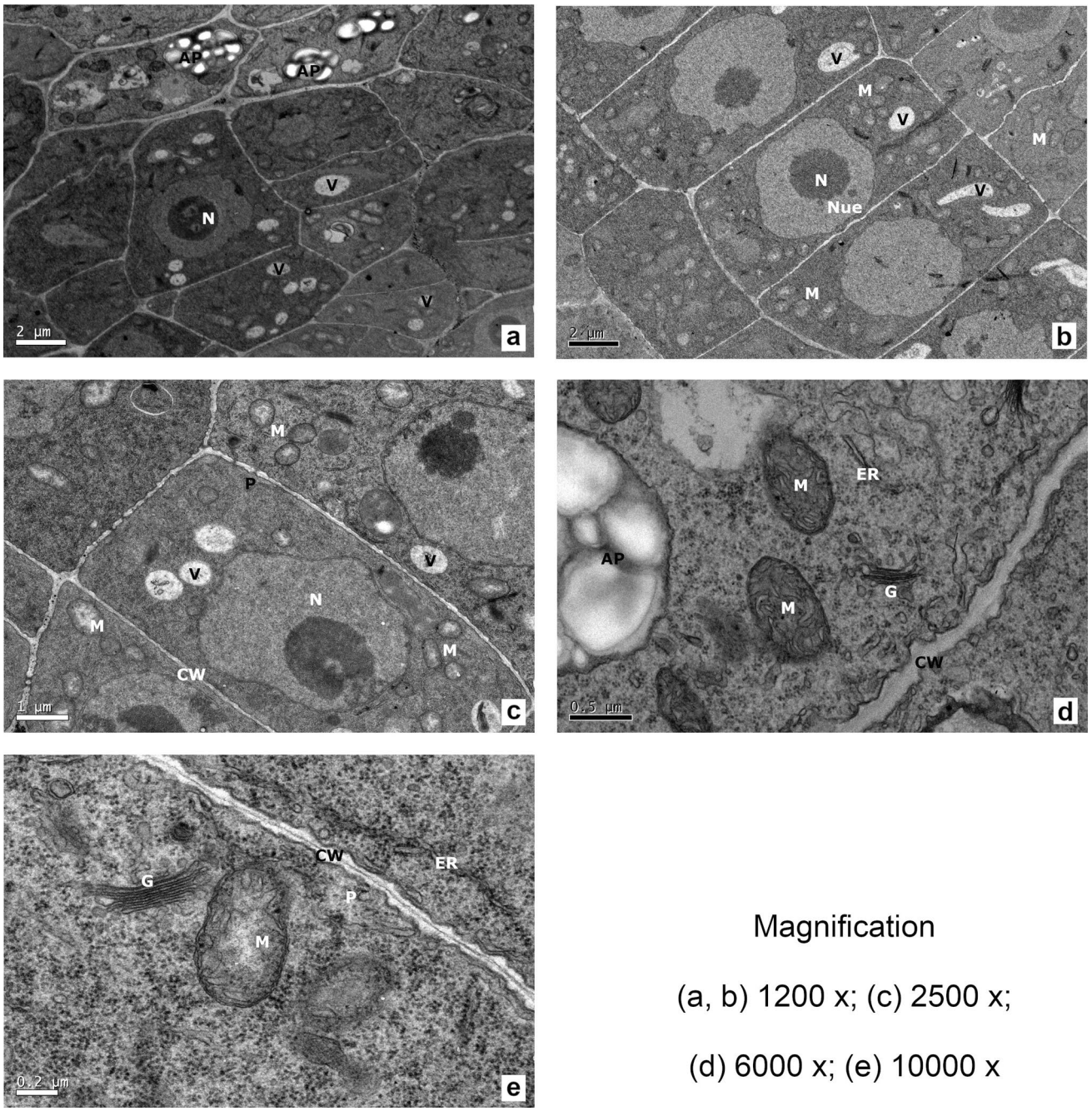

Fig. 6 TEM micrographs of root tip cells from *A. thaliana* (Control) grown for 15 days, showing features similar to those of 7-day-old root tip cells regarding the format of complete cell, nuclei (**a**–**c**), the number and shapes of mitochondria and vacuoles (**a**–**c**), endoplasmic reticulum (**d**, **e**), Golgi apparatus (**d**, **e**), cell wall with plasmodesmata (**c**), and amyloplasts (**a**). *AP* Amyloplasts, *CW* cell wall, *ER* endoplasmic reticulum, *G* Golgi apparatus, *M* mitochondria, *Nue* nucleoli, *N* nucleus, *V* vacuoles, *Ve* vesicles, *P* plasmodesmata

mitochondria. In 15-day-old TAA-treated cells, it was also found enlarged mitochondria with irregular shapes, but no evidence of broken mitochondria or significant changes in their cristae stromal translucency. In both 7- and 15-day-old TAA-treated seedlings no significant change was observed in the cell format, their nuclei, and in the endoplasmic reticulum and the Golgi apparatus when compared with untreated ones.

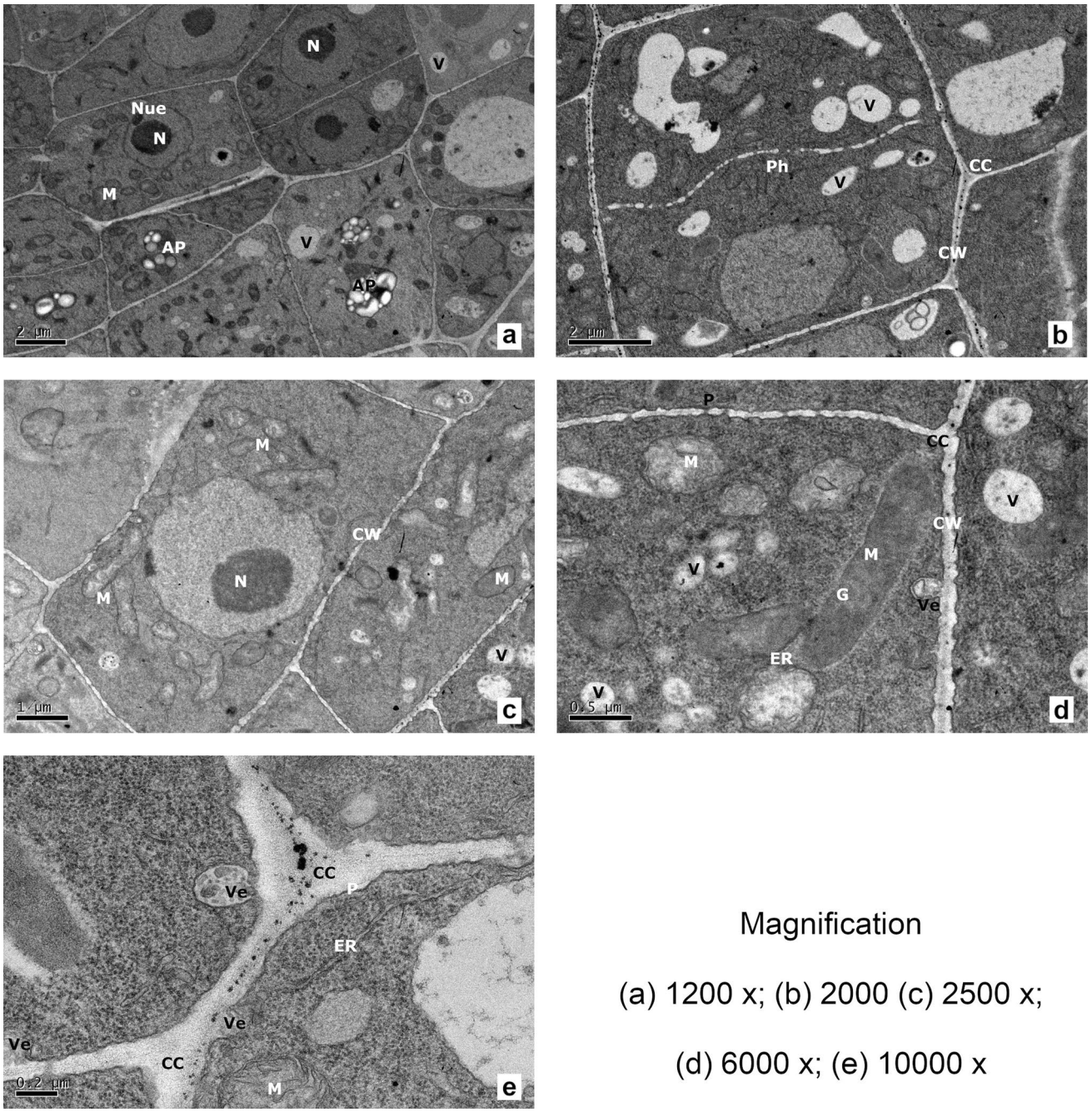

Fig. 7 TEM micrograph of root tip cells of *A. thaliana* grown for 7 days in the presence of IC_{50} *trans*-aconitic acid, showing a complete cell with nucleus not significantly different from that of untreated ones (**a**), amyloplasts (**a**), increased number of mitochondria and vacuoles (**a**–**d**), presence of cell phragmoplast (**b**), mitochondria with various sizes (**c**), including a huge and extended mitochondria (**d**), swollen cell corners with accumulation of electron-dense deposits (**e**), numerous vesicles in the plasma membrane/cell wall interspace (**d**, **e**), vacuoles containing dense granulose material and some of them with irregular shapes (**c**, **d**). *AP* Amyloplasts, *CC* cell corners, *CW* cell wall, *ER* endoplasmic reticulum, *M* mitochondria, *Nue* nucleoli, *N* nucleus, *V* vacuoles, *Ve* vesicles, *Ph* phragmoplast, *P* plasmodesmata

Discussion

This study revealed that the exogenous application of TAA at a concentration range of 400–1200 µM exerted significant changes in the development of *A. thaliana* seedlings, with a pronounced alteration of root architecture. Despite a substantial reduction in primary root length, the TEM images of root tips of seedlings grown in the presence of TAA at

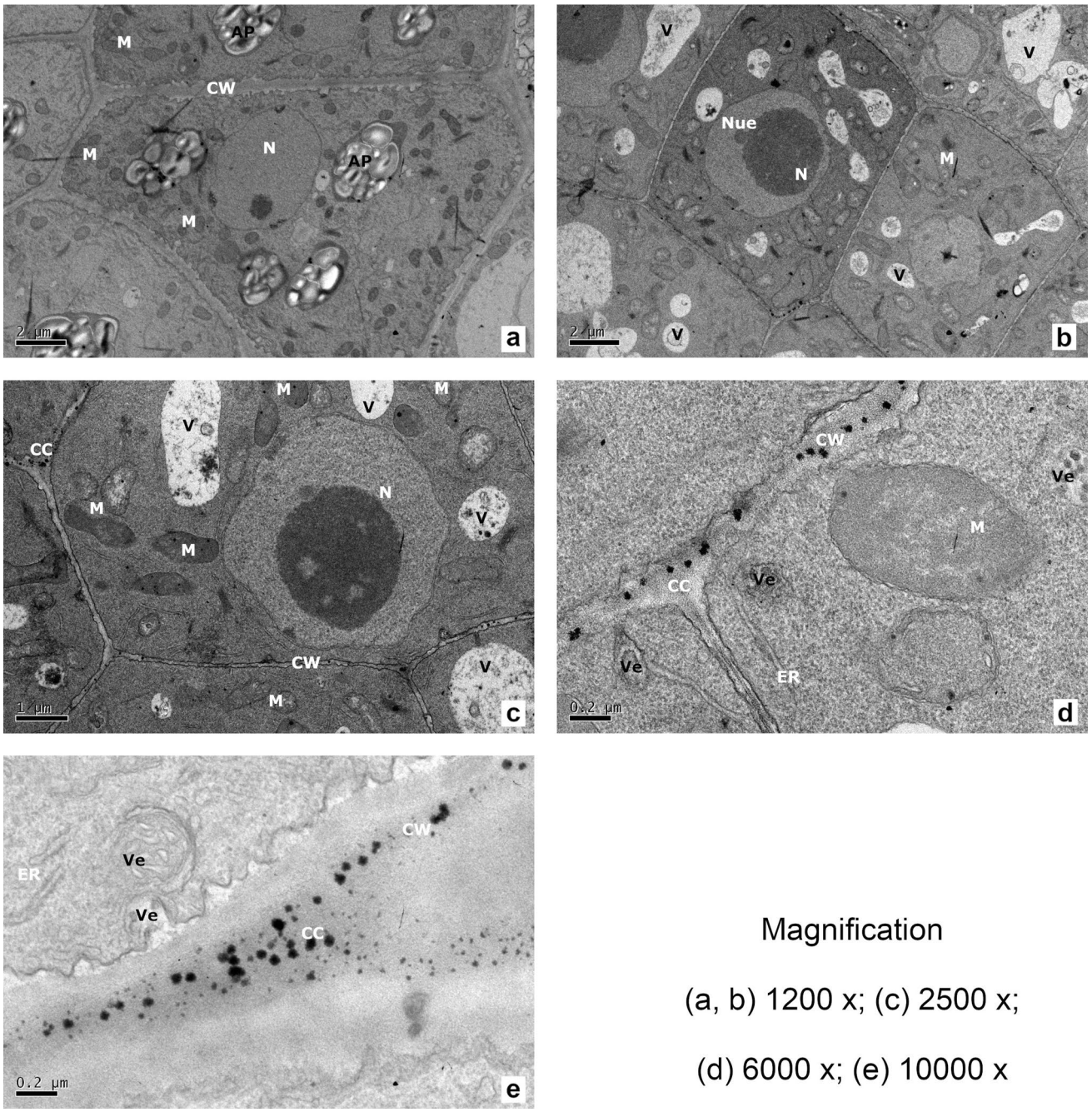

Fig. 8 TEM micrograph of root tip cells of *A. thaliana* grown for 15 days in the presence of IC_{50} *trans*-aconitic acid, showing a complete cell with an increased number of mitochondria (**a**, **b**), presence of amyloplasts (**a**), and no significant differences in the nuclei (**b**, **c**) compared with those from untreated cells, enlarged vacuoles containing electron-dense material (**b**, **c**), enlarged mitochondria with irregular shapes (**c**, **d**), membrane-bound structures containing granulose material (**d**, **e**), swollen cell corners with accumulation of electron-dense deposits (be); vesicles in the plasma membrane/cellwall interspace containing granulose material (**d**, **e**). *AP* Amyloplasts, *CC* cell corners, *CW* cell wall, *ER* endoplasmic reticulum, *G* Golgi apparatus, *M* mitochondria, *Nue* nucleoli, *N* nucleus, *V* vacuoles, *Ve* vesicles

the IC_{50} concentration (684 µM) did not reveal structural disorganization of the cell layers or the presence of hypertrophic or ruptured cells, alterations normally found under cell death conditions (Burgos et al. 2004; Ishii-Iwamoto et al. 2012; Diaz-Tielas et al. 2012). Apparently, there was no cellular energy deficit, since the growth of aerial parts of *A. thaliana* seedlings grown in the presence of 400–800 µM TAA was not significantly altered. However, a predominance

of cytotoxic effects was observed at the highest dose of 1200 µM TAA, with a substantial reduction in the development of both roots and aerial parts of the seedlings.

The morphological and ultrastructural changes of *A. thaliana* seedlings at lower doses of TAA are, most probably, reflecting the direct effects of TAA and the adaptive responses of cells to higher TAA accumulation in the cells. TAA caused a reduction of the distance between the meristematic zone and the zone of lateral roots formation, with precocious appearance of lateral roots and root hairs just above the root apex. These findings suggest a premature exit of cells from the meristematic zone, probably due to the loss of quiescent center identity, an action similar to that induced by farnese in *A. thaliana* (Araniti et al. 2017). These changes suggest an interference in the homeostasis of hormones that act in an integrated way in the development of the root system, including auxins, cytokinins, abscisic acid, ethylene and gibberellins (Clouse and Sasse 1998; Depuydt and Hardtke 2011; Ubeda-Tomás et al. 2012; Pacifici et al. 2015; Araniti et al. 2017).

It seems that TAA interfered with the development of *A. thaliana* as many natural and artificial substances that act in a similar mode to the exogenous auxins. In general, these auxinic compounds induce elongation of primary roots in low concentrations and/or inhibition in higher concentrations, promote the growth of stems, lateral/adventitious roots, and root hair, and facilitate root gravitropism (Casimiro et al. 2003; Benková et al. 2003; Laskowski et al. 2006; Pelagio-Flores et al. 2012; Pacurar et al. 2014; Wang et al. 2016). The regulatory actions of auxin on root development depend on the reactions of the synthesis, conjugation, transport, signaling, and/or metabolization (Diekmann et al. 1995; Friml et al. 2003; Cheng et al. 2007), defining the effective concentrations of auxins in different zones of the primary roots along its longitudinal axis (Swarup et al. 2005; Verbelen et al. 2006; Wang et al. 2016). The auxins can be protonated or deprotonated depending on the pH and these state of protonation alter their affinity to transporters or receptors and the diffusability across membranes (Swarup et al. 2005; Verbelen et al. 2006; Hachiya et al. 2014; Wang et al. 2016). It seems plausible that changes in the pH of different parts of root tissues play a role in the mode of action of TAA in *A. thaliana*. As a low molecular organic acid, the exogenous TAA may penetrate and accumulate in many parts of the root tissues, changing the local pH. By crossing the cell plasma membrane in the undissociated form, TAA can lead to a decrease in the internal cell pH when protons are internally released, which can also result in TAA accumulation in the dissociated form (Piper et al. 2001; Klasson 2017). Thus, the effects of TAA on root development may be, partly at least, mediated by changes in IAA distribution, an action secondary to TAA-induced changes in the pH in root tissues.

Access of TAA to various tissues and cell compartments was evidenced by TEM images, showing an increase in the vacuoles and membrane vesicles in TAA-treated seedlings. It is known that organic acids such as malate and citrate are accumulated in the vacuole, reaching concentrations 1 to 10-fold higher than in the cytosol, a process favored by low vacuolar pH values (Osmond 1976; Chang and Roberts 1991; Gout et al. 1993). The increase in the number and volume of vacuoles, along with the deposition of dense materials observed in TEM images, may represent a mechanism to prevent excessive TAA in the cytosol and mitochondria, forcing it into a limited area. Besides accumulation in vacuoles, TEM images showed vesicles derived from the invaginations of plasmalemma also containing dense materials and electron-dense granules attached to the cell wall. These findings suggest active apoplastic and symplastic movements of TAA in the roots of *A. thaliana*, changing the pH of various tissue compartments.

The accumulation of large amounts of TAA in the vesicles and/or in the cell wall was possibly favored because of its ability to chelate intracellular cations such as Ca^{2+}, Mn^{2+}, Mg^{+2}, or Fe^{2+}. This property is the basis of the exudation of many organic acids such as malate, malonate, citrate, and aconitate from the roots to the soil to favor nutrient acquisition and to protect plants against metal detoxification (Jones 1998). The binding of TAA with magnesium is also the cause of the grass tetany syndrome in ruminants (Thompson et al. 1997). It seems that electron-dense particles, seen in vacuoles, vesicles and cell walls were derived from insoluble salts of TAA with cellular cations. This accumulation of substances outside cells usually represents a protective mechanism of the cells to foreign or self-produced substances, a phenomenon that has been observed in the protection against poisoning ions such as cadmium (Khan et al. 1984) and lead (Phang et al. 2011).

The vacuolar and cell wall accumulation of TAA may play a role in the tolerance of *A. thaliana* to TAA at concentrations lower than 1000 µM. By preventing the circulation of excessive free TAA in the cytosol and mitochondria, the inhibition of mitochondrial and cytosolic aconitase could be prevented (Saffran and Prado 1949; Eprintsev et al. 2015). This assumption is in accordance with the lack of signs of metabolic disturbances in TAA-treated seedlings. Under an energy deficit condition, numerous disturbances in the cellular ultrastructure are expected, such as in chalcone-treated *A. thaliana* roots (Diaz-Tielas et al. 2012), in which the cells become irregular, swollen, and deformed, and the different zones cannot be longer distinguished in the apical meristem. Besides not exhibiting such alterations, many signs of energy-dependent processes were observed in TAA-treated cells, including an active cell and mitochondria division seen in TEM images of root tips and the development of numerous lateral roots.

The mechanisms of intra- and extracellular accumulation of TAA must be kinetically controlled and dependent on exogenous concentrations of TAA. Possibly, at a higher concentration of 1200 µM, these mechanisms reached saturation as the development of *A. thaliana* was strongly inhibited. Under this condition, free TAA may reach concentrations inhibitory to aconitase. The inhibition of mitochondrial aconitase by TAA is higher than that of cytosolic aconitase, and thus, the citrate may be directed to isocitrate formation in the cytosol, disturbing TCA functioning (Eprintsev et al. 2015). Magnesium is an essential cofactor for aconitase activity, and the binding of free magnesium by TAA also contributes to aconitase inhibition (Blair 1969). Other enzymes dependent on Mg^{2+} or other cations, such as Ca^{2+}, may also be affected by TAA at a higher concentration. Therefore, besides mitochondrial energy metabolism, a systemic metabolic dysfunction could be expected.

The equilibrium between cellular protection and cytotoxicity against exogenous TAA likely depends on the species. In *Glycine max* L., Coelho-Bortolo et al. (2018) observed alterations in root growth at TAA concentrations higher than 2000 µM and alteration of photosynthetic parameters only at concentrations higher than 7500 µM. In the weed species *I. grandifolia*, TAA inhibits seedling growth in a concentration range of 30–300 µM (Foletto et al. 2012), i.e., well above the cytotoxic concentrations in *Glycine max*. TAA seems to interfere with weeds at concentrations well below those toxic to crops.

Conclusions

The data presented here reveal that the roots of *A. thaliana* are highly sensitive to exogenous TAA. The alterations in the root morphology and ultrastructure were suggestive of adaptive responses to exclude free TAA from the cytosolic and mitochondrial space, thus preserving cell metabolism. The movements of TAA from the external medium into the cells probably changed the pH along the primary root, affecting the actions of auxins, as suggested by the early appearance of lateral roots and root hairs. At concentrations higher than 1000 µM, the adaptive responses seem not be longer effective leading to cytotoxic effects. Besides contributing to an understanding of the mode of exogenous TAA action on initial seedling growth, the results of the present work highlight the potential of TAA and also of cover plants rich in TAA, such as sweet sorghum and *Urochloa,* to reduce weed infestations. A decrease in weed competitiveness due to the actions of a natural compound can contribute to minimize crop yield losses and to decrease the use of synthetic herbicides.

Author contributions statement AMS-M, MJR and ELI-I contributed to the study conception and design. Material preparation, data collection and analysis were performed by KAK-C and MSM. The first draft of the manuscript was written by ELI-I and all authors commented on previous versions of the manuscript. All authors read and approved the final manuscript.

Acknowledgements The authors gratefully to Jesús Méndez and Guadalupe Casal of Center Research Services at the University of Vigo (CACTI) for technical assistance in microscopy. This research was supported by Project number AGL2013-41281-R from the Spanish Ministry of Economy and Competitiveness. Kátia Aparecida Kern-Cardoso fellowship holder from the Coordination for the Improvement of Higher Education Personnel (CAPES).

Funding Open Access funding provided thanks to the CRUE-CSIC agreement with Springer Nature. The study was funding by Spanish Ministry of Economy and from the Coordination for the Improvement of Higher Education Personnel (CAPES) Brazil.

Availability of data and materials The datasets generated during and/or analyzed during the current study are available from the corresponding author on reasonable request.

Code availability Not applicable.

Declarations

Conflict of interest Author Adela María Sánchez-Moreiras has received research grants from Spanish Ministry of Economy and Competitiveness (Project number AGL2013-41281-R). Kátia Aparecida Kern-Cardoso has received a doctorate-sandwich scholarship from the Coordination for the Improvement of Higher Education Personnel (CAPES).

Ethics approval Not applicable.

Open Access This article is licensed under a Creative Commons Attribution 4.0 International License, which permits use, sharing, adaptation, distribution and reproduction in any medium or format, as long as you give appropriate credit to the original author(s) and the source, provide a link to the Creative Commons licence, and indicate if changes were made. The images or other third party material in this article are included in the article's Creative Commons licence, unless indicated otherwise in a credit line to the material. If material is not included in the article's Creative Commons licence and your intended use is not permitted by statutory regulation or exceeds the permitted use, you will need to obtain permission directly from the copyright holder. To view a copy of this licence, visit http://creativecommons.org/licenses/by/4.0/.

References

Araniti F, Bruno L, Sunseri F, Pacenza M, Forgione I, Bitonti MB, Abenavoli MR (2017) The allelochemical farnesene affects *Arabidopsis thaliana* root meristem altering auxin distribution. Plant Physiol Biochem 121:14–20. https://doi.org/10.1016/j.plaphy.2017.10.005

Benková E, Michniewicz M, Sauer M, Teichmann T, Seifertová D, Jürgens G, Friml J (2003) Local, efflux-dependent auxin gradients as a common module for plant organ formation. Cell 115:591–602. https://doi.org/10.1016/S0092-8674(03)00924-3

Blair JM (1969) Magnesium and the aconitase equilibrium: determination of apparent stability constants of magnesium substrate complexes from equilibrium data. Eur J Biochem 8:287–291. https://doi.org/10.1111/j.1432-1033.1969.tb00526.x

Brauer D, Teel MR (1981) Metabolism of *trans*-aconitic acid in maize. Plant Physiol 68:1406–1408. https://doi.org/10.1104/pp.68.6.1406

Brauer D, Teel MR (1982) Metabolism of *trans*-aconitic acid in maize. Plant Physiol 70:723–727. https://doi.org/10.1104/pp.70.3.723

Brum KB, Haraguchi M, Garutti MB, Nóbrega FN, Rosa B, Fioravanti MCS (2009) Steroidal saponin concentrations in *Brachiaria decumbens* and *B. brizantha* at different developmental stages. Ciência Rural 39:279–281. https://doi.org/10.1590/S0103-84782008005000034

Burgos NR, Talbert RE, Kim KS, Kuk YI (2004) Growth inhibition and root ultrastructure of cucumber seedlings exposed to allelochemicals from rye (*Secale cereale*). J Chem Ecol 30:671–689. https://doi.org/10.1023/B:JOEC.0000018637.94002.ba

Casimiro I, Beeckman T, Graham N, Bhalerao R, Zhang H, Casero P, Sandberg G, Bennett MJ (2003) Dissecting *Arabidopsis* lateral root development. Trends Plant Sci 8:165–171. https://doi.org/10.1016/S1360-1385(03)00051-7

Chang K, Roberts JKM (1991) Cytoplasmic malate levels in maize root tips during K^+ ion uptake determined by ^{13}C-NMR spectroscopy. Biochim Biophys Acta Mol Cell Res 1092:29–34. https://doi.org/10.1016/0167-4889(91)90174-V

Cheng Y, Dai X, Zhao Y (2007) Auxin synthesized by the YUCCA flavin monooxygenases is essential for embryogenesis and leaf formation in *Arabidopsis*. Plant Cell 19:2430–2439. https://doi.org/10.1105/tpc.107.053009

Clouse SD, Sasse JM (1998) Brassinosteroids: essential regulators of plant growth and development. Annu Rev Plant Physiol Plant Mol Biol 49:427–451. https://doi.org/10.1146/annurev.arplant.49.1.427

da Coelho-Bortolo TS, Marchiosi R, Viganó J, de Siqueira-Soares RC, Ferro AP, Barreto GE, de Bido GS, Abrahão J, dos Santos WD, Ferrarese-Filho O (2018) *Trans*-aconitic acid inhibits the growth and photosynthesis of *Glycine max*. Plant Physiol Biochem 132:490–496. https://doi.org/10.1016/j.plaphy.2018.09.036

Depuydt S, Hardtke CS (2011) Hormone signalling crosstalk in plant growth regulation. Curr Biol 21:R365–R373. https://doi.org/10.1016/j.cub.2011.03.013

Diaz-Tielas C, Grana E, Sotelo T, Reigosa MJ, Sanchez-Moreiras AM (2012) The natural compound trans-chalcone induces programmed cell death in *Arabidopsis thaliana* roots. Plant Cell Environ 35:1500–1517. https://doi.org/10.1111/j.1365-3040.2012.02506.x

Diekmann W, Venis MA, Robinson DG (1995) Auxins induce clustering of the auxin-binding protein at the surface of maize coleoptile protoplasts. Proc Natl Acad Sci 92:3425–3429. https://doi.org/10.1073/pnas.92.8.3425

Dorman D, Madsen L, Day D (2015) Aconitic acid: old compound, new uses. Macromol Symp 351:87–89. https://doi.org/10.1002/masy.201400139

Du C, Cao S, Shi X, Nie X, Zheng J, Deng Y, Ruan L, Peng D, Sun M (2017) Genetic and biochemical characterization of a gene operon for *trans*-aconitic acid, a novel nematicide from *Bacillus thuringiensis*. J Biol Chem 292:3517–3530. https://doi.org/10.1074/jbc.M116.762666

Eprintsev AT, Fedorin DN, Nikitina MV, Igamberdiev AU (2015) Expression and properties of the mitochondrial and cytosolic forms of aconitase in maize scutellum. J Plant Physiol 181:14–19. https://doi.org/10.1016/J.JPLPH.2015.03.012

Foletto MP, Kagami F, Voll E, Kern-Cardoso KA, Pergo-Coelho EM, Rocha M, Silva AA, Sarragiotto MH, Ishii-Iwamoto EL (2012) Allelopathic effects of *Brachiaria ruziziensis* and aconitic acid on *Ipomoea triloba* weed. Allelopathy J 30:33–48

Friml J, Vieten A, Sauer M, Weijers D, Schwarz H, Hamann T, Offringa R, Jürgens G (2003) Efflux-dependent auxin gradients establish the apical–basal axis of *Arabidopsis*. Nature 426:147–153. https://doi.org/10.1038/nature02085

Gout E, Bligny R, Pascal N, Douce R (1993) ^{13}C nuclear magnetic resonance studies of malate and citrate synthesis and compartmentation in higher plant cells. J Biol Chem 268:3986–3992. https://doi.org/10.1016/S0021-9258(18)53568-7

Hachiya T, Sugiura D, Kojima M, Sato S, Yanagisawa S, Sakakibara H, Terashima I, Noguchi K (2014) High CO_2 triggers preferential root growth of *Arabidopsis thaliana* via two distinct systems under low pH and low N stresses. Plant Cell Physiol 55:269–280. https://doi.org/10.1093/pcp/pcu001

Ishii-Iwamoto EL, Pergo Coelho EM, Reis B, Moscheta IS, Bonato CM (2012) Effects of monoterpenes on physiological processes during seed germination and seedling growth. Curr Bioact Compd 8:50–64. https://doi.org/10.2174/157340712799828223

Jones DL (1998) Organic acids in the rhizosphere – a critical review. Plant Soil 205:25–44. https://doi.org/10.1023/A:1004356007312

Katsuhara M, Sakano K, Sato M, Kawakita H, Kawabe S (1993) Distribution and production of *trans*-aconitic acid in Barnyard Grass (*Echinochloa crus-galli* var. oryzicola) as putative antifeedant against brown planthoppers. Plant Cell Physiol 34:251–254. https://doi.org/10.1093/oxfordjournals.pcp.a078414

Kellermeier F, Armengaud P, Seditas TJ, Danku J, Salt DE, Amtmann A (2014) Analysis of the root system architecture of *Arabidopsis* provides a quantitative readout of crosstalk between nutritional signals. Plant Cell 26:1480–1496. https://doi.org/10.1105/tpc.113.122101

Khan DH, Duckett JG, Frankland B, Brian Kirkham J (1984) An x-ray microanalytical study of the distribution of cadmium in roots of *Zea mays* L. J Plant Physiol 115:19–28. https://doi.org/10.1016/S0176-1617(84)80047-4

Kidd PS, Llugany M, Poschenrieder C, Gunsé B, Barceló J (2001) The role of root exudates in aluminium resistance and silicon-induced amelioration of aluminium toxicity in three varieties of maize (*Zea mays* L.). J Exp Bot 52:1339–1352. https://doi.org/10.1093/jexbot/52.359.1339

Klasson KT (2017) Impact of potential fermentation inhibitors present in sweet sorghum sugar solutions. Sugar Tech 19:95–101. https://doi.org/10.1007/s12355-016-0433-2

Klinman JP, Rose IA (1971) Purification and kinetic properties of aconitate isomerase from *Pseudomonas putida*. Biochemistry 10:2253–2259. https://doi.org/10.1021/bi00788a011

Krogh A (1971) The content of trans-aconitic acid in *Asarum europaeum* L. determined by means of a chromatogram spectrophotometer. Acta Chem Scand 25:1495–1496. https://doi.org/10.3891/acta.chem.scand.25-1495

Laskowski M, Biller S, Stanley K, Kajstura T, Prusty R (2006) Expression profiling of auxin-treated *Arabidopsis* roots: toward a molecular analysis of lateral root emergence. Plant Cell Physiol 47:788–792. https://doi.org/10.1093/pcp/pcj043

Mariano ED, Keltjen WG (2003) Evaluating the role of root citrate exudation as a mechanism of aluminium resistance in maize genotypes. Plant Soil 256:469–479. https://doi.org/10.1023/A:1026106714644

Müller M, Schmidt W (2004) Environmentally induced plasticity of root hair development in *Arabidopsis*. Plant Physiol 134:409–419. https://doi.org/10.1104/pp.103.029066

Osmond CB (1976) Ion absorption and carbon metabolism in cells of higher plants. In: Pitman MG, Lüttge U (eds) Transport in plants II. Springer Berlin Heidelberg, Berlin, pp 347–372

Pacifici E, Polverari L, Sabatini S (2015) Plant hormone cross-talk: the pivot of root growth. J Exp Bot 66:1113–1121. https://doi.org/10.1093/jxb/eru534

Pacurar DI, Perrone I, Bellini C (2014) Auxin is a central player in the hormone cross-talks that control adventitious rooting. Physiol Plant 151:83–96. https://doi.org/10.1111/ppl.12171

Pang PP, Meyerowitz EM (1987) *Arabidopsis thaliana*: a model system for plant molecular biology. Nat Biotechnol 5:1177–1181. https://doi.org/10.1038/nbt1187-1177

Pelagio-Flores R, Muñoz-Parra E, Ortiz-Castro R, López-Bucio J (2012a) Melatonin regulates *Arabidopsis* root system architecture likely acting independently of auxin signaling. J Pineal Res 53:279–288. https://doi.org/10.1111/j.1600-079X.2012.00996.x

Petersson SV, Johansson AI, Kowalczyk M, Makoveychuk A, Wang JY, Moritz T, Grebe M, Benfey PN, Sandberg G, Ljung K (2009) An auxin gradient and maximum in the *Arabidopsis* root apex shown by high-resolution cell-specific analysis of IAA distribution and synthesis. Plant Cell 21:1659–1668. https://doi.org/10.1105/tpc.109.066480

Phang IC, Leung DWM, Taylor HH, Burritt DJ (2011) Correlation of growth inhibition with accumulation of Pb in cell wall and changes in response to oxidative stress in *Arabidopsis thaliana* seedlings. Plant Growth Regul 64:17–25. https://doi.org/10.1007/s10725-010-9527-0

Piper P, Calderon CO, Hatzixanthis K, Mollapour M (2001) Weak acid adaptation: the stress response that confers yeasts with resistance to organic acid food preservatives. Microbiology 147:2635–2642. https://doi.org/10.1099/00221287-147-10-2635

Rahman A, Hosokawa S, Oono Y, Amakawa T, Goto N, Tsurumi S (2002) Auxin and ethylene response interactions during *Arabidopsis* root hair development dissected by auxin influx modulators. Plant Physiol 130:1908–1917. https://doi.org/10.1104/pp.010546

Rémus-Borel W, Shallow N, McNally DJ, Labbé C, Bélanger RR (2006) High-speed counter-current chromatography for the study of defense metabolites in wheat. J Chromatogr A 1121:200–208. https://doi.org/10.1016/j.chroma.2006.04.004

Rémus-Borel W, Menzies JG, Bélanger RR (2009) Aconitate and methyl aconitate are modulated by silicon in powdery mildew-infected wheat plants. J Plant Physiol 166:1413–1422. https://doi.org/10.1016/j.jplph.2009.02.011

Reynolds ES (1963) The use of lead citrate at high pH as an electron-opaque stain in electron microscopy. J Cell Biol 17:208–212. https://doi.org/10.1083/jcb.17.1.208

Saffran M, Prado JL (1949) Inhibition of aconitase by *trans*-aconitate. J Biol Chem 180:1301–1309

Sánchez-Moreiras AM, Graña E, Díaz-Tielas C, López-González D, Araniti F, Celeiro M, Teijeira M, Verdeguer M, Reigosa MJ (2018) Elucidating the phytotoxic potential of natural compounds. In: Sánchez-Moreiras AM, Reigosa MJ (eds) Advances in plant ecophysiology techniques. Springer International Publishing, Cham, pp 363–378

Swarup R, Kramer EM, Perry P, Knox K, Leyser HMO, Haseloff J, Beemster GTS, Bhalerao R, Bennett MJ (2005) Root gravitropism requires lateral root cap and epidermal cells for transport and response to a mobile auxin signal. Nat Cell Biol 7:1057–1065. https://doi.org/10.1038/ncb1316

Thompson JF, Schaefer SC, Madison JT (1990) Determination of aconitate isomerase in plants. Anal Biochem 184:39–47. https://doi.org/10.1016/0003-2697(90)90008-W

Thompson JF, Schaefer SC, Madison JT (1997) Role of aconitate isomerase in *trans*-aconitate accumulation in plants. J Agric Food Chem 45:3684–3688. https://doi.org/10.1021/jf970131s

Ubeda-Tomás S, Beemster GTS, Bennett MJ (2012) Hormonal regulation of root growth: integrating local activities into global behaviour. Trends Plant Sci 17:326–331. https://doi.org/10.1016/j.tplants.2012.02.002

Verbelen J-P, De CT, Le J, Vissenberg K, Baluška F (2006) The root apex of *Arabidopsis thaliana* consists of four distinct zones of growth activities. Plant Signal Behav 1:296–304. https://doi.org/10.4161/psb.1.6.3511

Voll E, Franchini JC, Da Cruz RT, Gazziero DLP, Brighenti AM, Adegas FS (2004) Chemical Interactions of *Brachiaria plantaginea* with *Commelina bengalensis* and A*canthospermum hispidum* in Soybean Cropping Systems. J Chem Ecol 30:1467–1475. https://doi.org/10.1023/B:JOEC.0000037752.57907.fb

Voll E, Gazziero DLP, Adegas FS (2010) Ácido aconítico em sementes de espécies de plantas daninhas de diferentes locais. Planta Daninha 28:13–22. https://doi.org/10.1590/S0100-83582010000100002

Wang Q, An B, Wei Y, Reiter RJ, Shi H, Luo H, He C (2016) Melatonin regulates root meristem by repressing auxin synthesis and polar auxin transport in *Arabidopsis*. Front Plant Sci 7:1882. https://doi.org/10.3389/fpls.2016.01882

Wenzl P, Chaves AL, Patiño GM, Mayer JE, Rao IM (2002) Aluminum stress stimulates the accumulation of organic acids in root apices of Brachiaria species. J Plant Nutr Soil Sci 165:582–588. https://doi.org/10.1002/1522-2624(200210)

Williamson LC, Ribrioux SPCP, Fitter AH, Leyser HMO (2001) Phosphate availability regulates root system architecture in *Arabidopsis*. Plant Physiol 126:875–882. https://doi.org/10.1104/pp.126.2.875

Yuhara K, Yonehara H, Hattori T, Kobayashi K, Kirimura K (2015) Enzymatic characterization and gene identification of aconitate isomerase, an enzyme involved in assimilation of *trans*-aconitic acid, from *Pseudomonas* sp. WU-0701. FEBS J 282:4257–4267. https://doi.org/10.1111/febs.13494

Publisher's Note Springer Nature remains neutral with regard to jurisdictional claims in published maps and institutional affiliations.